

# IDENTIFICATION OF NOVEL MAP4K4 INHIBITORS THROUGH QSAR, DOCKING, MOLECULAR DYNAMICS SIMULATIONS AND FREE ENERGY STUDIES

**Dorka VijayaKumari Beri\***

<sup>a</sup>Dept. of Biotechnology, VFSTR Deemed to be University, Vadlamudi, Andhra Pradesh, 522213

<sup>b</sup>Govt. College for Women (A), Sambasiva Pet, Guntur, Andhra Pradesh 522001

Contact No: 99639 28874

Email:[dorca.vj@gmail.com](mailto:dorca.vj@gmail.com)

\*Corresponding Author

**Krupanidhi Srirama**

<sup>a</sup>Dept. of Biotechnology, VFSTR Deemed to be University, Vadlamudi, Andhra Pradesh, 522213

[krupanidhi.srirama@gmail.com](mailto:krupanidhi.srirama@gmail.com)

## IDENTIFICATION OF NOVEL MAP4K4 INHIBITORS THROUGH QSAR, DOCKING, MOLECULAR DYNAMICS SIMULATIONS AND FREE ENERGY STUDIES

### ABSTRACT

Mitogen-activated protein 4 kinase 4 (MAP4K4) is a serine/threonine kinase involved in various signaling pathways. Overexpression of MAP4K4 plays an important role in different cancers and became an attractive therapeutic target for cancer. The pyridopyrimidine-based structural core analogs as novel MAP4K4 inhibitors have been performed by using the QSAR model generation program 'Ezqsar'. A total of 26 molecules with wide range of activities was divided into training set and test set, were used to build the QSAR model and to validate the model. The best QSAR model generated from the training set has the regression square value ( $r^2$ ) 0.92, and the validation ( $q^2$ ) has the value of 0.84. The molecules from GSK-PKIS database as external set was used to predict the activity using the QSAR model and two of them found to have good predicted inhibitory values. Molecular docking, molecular dynamics simulations and mmpbsa free energy calculations of high and low active molecules and two QSAR predicted active molecules (M1 and M8) with MAP4K4 protein revealed the key interaction in molecule binding.

**Graphical Abstract here**

**Keywords:** Pyridopyrimidine, MAP4K4, QSAR, Docking, MD simulations, Ezqsar.

### 1. INTRODUCTION

Mitogen-activated protein kinases (MAPK) play a vital role in cell activation, differentiation, proliferation and apoptosis. The upstream activators of MAP3Ks are GTP-protein binders. However, MAP3K is activated by MAP kinase kinase kinase (MAP4K) in various pathways (Chuang et al., 2016). There are six MAP4Ks belonging to the mammalian family of the Ste20-like serine/threonine kinase family because of their similarity with the budding yeast kinase Ste20p (sterile 20 proteins) (Wu et al., 1995). In MAP4Ks, the MAP4K4 is known as HGK (hepatocyte progenitor kinase-like/germinal center kinase-like kinase) or NIK (Nck-interacting kinase) (Su et al., 1997). Ste20-like kinases have two sub-families based on their domain structure, such as p21- activated kinases and the germinal center kinases (Delpire, 2009). Further MAP4K4 belongs to the mammalian GCK-IV subfamily. Ste20 family kinases are associated with different types of signalling pathways. Precisely, the function of MAP4K4 is connected with numerous physiological processes as well as pathological conditions. This includes metabolisms, (Tang et al., 2006; Baumgartner et al., 2006; Bouzakri and Zierath, 2007; Bouzakri et al., 2009) inflammation, (Aouadi et al., 2009) neural degeneration (Loh et al., 2007) and cancer, (Wright et al., 2003; Collins et al., 2006; Liu et al., 2011; Liang et al., 2008; Qiu et al., 2012; Mao et al., 2006) which suggests that inhibition of MAP4K4 function, is beneficial in the treatment of diseases associated with the above processes. The preclinical and patient association studies strongly recommend that MAP4K4 plays a significant role in various types of cancers. Thus, the MAP4K4 could be a potential target for cancer treatment.

Previous studies show that MAP4K4 plays a vital role in many types of tumors. A negative association between patient prognosis and MAP4K4 expression was observed in various types of cancers. In the literature, it is evident that MAP4K4 served as a negative prognostic target in colorectal cancer treatment, (Hao et al., 2010) pancreatic ductal adenocarcinoma, (Liang et al., 2008) lung cancer (Qiu et al., 2012) and prostate cancer (Rizzardi et al., 2014) Insights into the mechanism of MAP4K4 functions have yet to be fully elucidated. Thus, a deeper understanding of this kinase role using small molecule inhibitors could provide essential MAP4K4 therapeutic applications. There are few studies on small molecule inhibitors for MAP4K4, fragment-based drug discovery tools to identify suitable inhibitors (Erlanson, 2011; Tanneeru et al., 2013; Tanneeru et al., 2012; Shanmukha et al., 2012; KrishnamRaju et al., 2018). In another study, pyridopyrimidine series molecules were identified with efficient inhibition capacity (Crawford et al., 2014). Further, in search of MAP4K4 inhibitors, a fragment-based study was carried out and found pyrrolotriazine series of molecules with good efficiency. Further modifications to this series using molecular modeling approaches led to identifying a more efficient pyrrolotriazine series of molecules (Wang et al., 2014; Purushotham, 2018; Purushotham and Sastry, 2014; Vadlakonda et al., 2017; Mehta and Pathak, 2017; Muttaqin et al., 2017; Ihsan and Yanuar, 2018).

In the absence of potent MAP4K4 inhibitors molecules, we have conducted a study to design efficient small molecule inhibitors with the help of Quantitative Structure Activity Relationship (QSAR) and molecular docking approaches. In this study, we aimed to develop a robust and efficient model for the inhibitory activity of small molecule MAP4K4 inhibitors. We used different methodologies to connect between structural parameters and MAP4K4 inhibition. These methods include QSAR using statistical analysis tool R-package software. A series of molecules are collected from the Crawford et al. study of selective 4-amino-pyridopyrimidine inhibitors of MAP4K4 kinase (Crawford et al., 2014) and presented QSAR analysis to ascertain the relationship between the structure and function of these inhibitors. The predicted active molecules from a database were further submitted to molecular docking into the MAP4K4 active site to gain deep understanding of the protein-ligand binding interactions. Molecular dynamics simulations of protein ligand complexes will reveal the stability of the ligand in the protein active site and the key residue interactions. The binding free energy calculations will help in understanding the ability of molecule binding in the active site. Our results in this study will aid in designing potential small molecule inhibitors of MAP4K4.

## 2. METHODOLOGY

### 2.1 QSAR model generation

Twenty-six molecules were collected from the literature along with their IC<sub>50</sub> values (Crawford et al., 2014). These molecules contain pyridopyrimidine series as core moiety. We have used an open-source software *Ezqsar* (Shamsara, 2017) which is developed with R (R: a language and environment for statistical computing) package, that could develop Multiple Linear Regression (MLR) QSAR models from 2D or 3D structures and their corresponding activities. R programming presents a flexible and open-source platform for statistical analyses (R Core Team, 2013). R programming presently constitutes the most common choice in drug discovery research for bioactivity estimation and druggable property modeling (Gentleman et al., 2004). In *Ezqsar*, descriptor generation is carried out with the help of a Chemistry Development Kit (CDK) library (Steinbeck et al., 2006). This program computes 2D and 3D descriptors. The molecular descriptor is physicochemical property parameters, which are used to correlate the molecule structure and their biological inhibitory property pIC<sub>50</sub>. The descriptors are classified into different groups such as topological, geometrical, constitutional and electronic. The 3D descriptors will be generated if the input structures are in the 3D coordinate format, otherwise, the descriptors for the molecule would be zero.

### 2.2 Model validation

The validation of the best QSAR model is achieved by the external and internal validation methods. The internal model quality cross validation  $r^2_{cv}$  (or  $q^2$ ) was measured by the leave-one-out (LOO) procedure (Fan et al., 2001). Significance of the relationship between the MAP4K4 kinase 2D or 3D structures with their pIC<sub>50</sub> values was obtained from this LOO of the QSAR model. In this study, a three-step-procedure for MLR was carried out which consisting of, i) Molecule sketching and minimization ii) Descriptor calculation and iii) MLR model generation. MLR method in QSAR studies is a popular, simple to use, highly reproducible method and the results can be easily interpretable (Roy et al., 2015; Roy et al., 2015). The quality of the best model is to predict the biological activity of the existing and other external set were achieved by using  $R^2$  and  $Q^2$  values. The square of regression (R) should be greater than 0.9 and the cross validation square (Q) should be greater than 0.5. Calculated predictivity of the generated best QSAR model is the square of  $R_{pred}$  should be greater than 0.6 is the standard acceptable value for the reliable model (Roy et al., 2015; Todeschini et al., 2016; Veerasamy et al., 2011).

### 2.3 Molecular docking studies

We have performed molecular docking of all inhibitors using Autodock4.2 software (Morris et al., 2009) into the 3D model of the MAP4K4 kinase domain. Autodock is a Genetic Algorithm (GA) based docking method used to perform flexible docking of inhibitors into protein binding sites. The Gasteiger partial charges were assigned to the small molecules and polar hydrogen atoms were added. The Autogrid was used to generate the grid maps on the protein active site. The grid was centered at the active site of the protein at  $-17.40 \times -3.37 \times 27.15 \text{ \AA}^3$  with grid dimensions of  $18 \times 18 \times 22 \text{ \AA}^3$  with points separated by  $1.0 \text{ \AA}$ . The Lamarckian genetic algorithm and other Autodock default parameters were used to perform the docking studies. After docking, the generated 20 ligand conformers were analyzed using Autodock Tools and python molecular viewer software to understand the mode of protein-inhibitor binding.

### 2.4 Molecular dynamics simulations and mmpbsa energy calculations

The protein ligand complexes molecular dynamics simulations were performed for 20 ns (nano seconds) under constant temperature and pressure conditions. All the MD simulations were performed by using Gromacs2018 version on Ubuntu 18.04 Linux flat form (Van Der Spoel et al., 2005). An edge length of  $10 \text{ \AA}$ , periodic cubic box around the protein ligand complexes constructed and solvent water molecules filled with simple point charge (SPC) water models. The complex negative charge was neutralized with 4  $\text{Na}^+$  ions. The steepest descent minimization of the protein ligand complex to get the initial stabilized structure and position restrained molecular dynamics for a 100 pico seconds (ps) to water molecule adjustment all over the system. Total 5 ns of molecular dynamics (MD) simulations performed or whole system using  $0.002 \text{ ps}$  time step. The V-rescale method thermostat (Bussi et al., 2007) was used for the constant temperature bath; the Parrinello-Rahman method (Parrinello and Rahman, 1981) was applied to maintain the 1 bar pressure all over the system. LINear Constraint Solver (LINCS) algorithm is used to constrain the hydrogen (Hess et al., 1997). Stabilized MD simulation trajectory files were extracted and utilized for the calculation of binding free energy. Molecular Mechanics Poisson-Boltzmann Surface Area (MMPBSA) free energy calculations were performed by using *mm\_pbsa* code in gromacs software (Kumari and Kumar R, 2014; Baker et al., 2001).

## 3. RESULTS

### 3.1 2D-QSAR study

For 2D-QSAR studies, a dataset of 4-Amino-pyridopyrimidine analog-based ATP-competitive inhibitors of MAP4K4 were used to generate a QSAR model. The activity of molecules was taken as pIC50 to generate the QSAR equation using the MLR method and was considered as dependent variable and the MLR descriptors were considered as independent variables. MLR method for regression analysis was carried out with the training set consisting of 21 compounds and the best model for training set molecules was developed using the MLR method. The best equation for the final analysis consisted of five terms and is shown below

$$\text{pIC50} = 7.15018057 - 7.62445357 (\text{Weta2.unitty}) + 15.69537370 * (\text{Weta3.unitty}) - 0.00282026 * (\text{ATSp4}) + 20.01026640 * (\text{ATSc4}) + 15.61763534 * (\text{ATSc5})$$

By using the CDK package, about 319 descriptors have been calculated for all 26 molecules. The program can generate the QSAR models using the descriptors with positive and negative coefficients and a constant. The best QSAR model is having a coefficient such as WHIM descriptors. The WHIM descriptors (Weta2.unitty, Weta3.unitty) are geometrical descriptors which are having the whole molecular structure information in the form of molecule size, shape, symmetry, and atom distribution. The Topological descriptor is Autocorrelation Polarizability order-4 descriptors (ATSp4). The other topological descriptors ATSc4 and ATSc5 are the Moreau-Broto autocorrelation descriptors using partial charges of the molecule. The 26 molecule set was divided randomly into a training set with 21 molecules and a test set with 5 molecules to generate the QSAR model. The training and test sets are having good, medium and low activity molecules. The activity spans between the highest active molecule 25 with pIC50 value 8.0 and lowest active molecule 17 with pIC50 value 5.23.



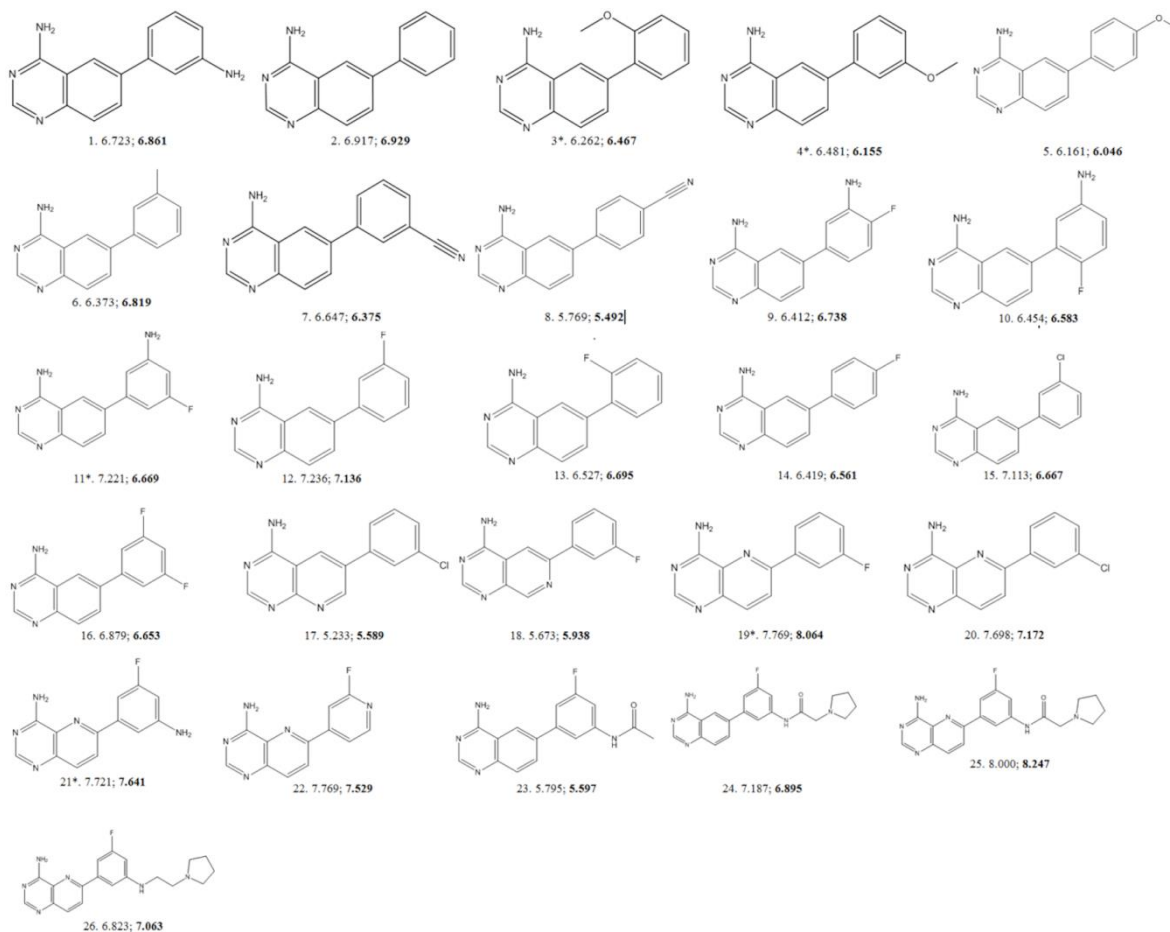


**Figure 1** : List of Training set & Test molecules with actual and predicted IC<sub>50</sub> values.

\*Test set molecules

The best QSAR model generated from the training set molecules is showing the regression square ( $r^2$ ) value 0.92. It is well known that the QSAR model regression value ( $r$ ) should be greater than 0.9, then it is considered as a reliable model. Internal validation of the model ( $q^2$ ) must be greater than or equal to 0.5. We obtained good  $q^2$  value of 0.84 for our model. The predicted  $r^2$  value should be greater than or equal to 0.6. We have obtained the  $r^2_{\text{predicted}}$  value of 0.81. From the results, it is evident that the generated model is a reliable model. The test set with five molecules predicted activity is tested on the model and the results are showing a good agreement with the actual activity. The predicted activities and the actual activities are shown in Fig. 1. The plot (Fig. 2) is the correlation between actual and predicted activities of training and test set molecules.

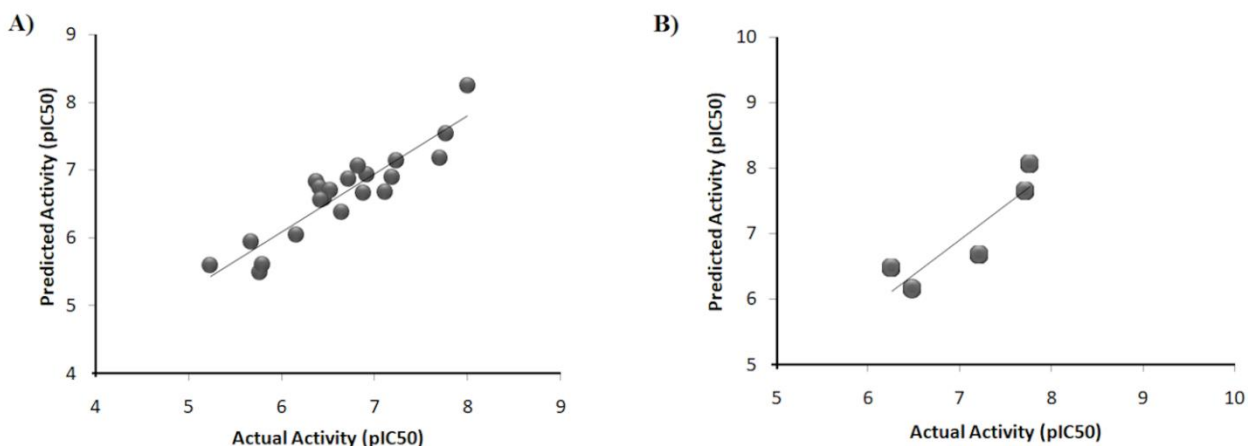


**Figure 2 :** The actual & predicted activity plot of A) Training set B) Test set molecules

The prediction of novel set molecules (external data set) activity by using the QSAR model was performed to find new inhibitors for MAP4K4. We have chosen a 367 molecules containing GSK-PKIS database as an external database. From the prediction of the molecules using the QSAR model, we have identified 10 molecules with similar core showing the activity pIC50 more than 7.5 (Figure-3). From the molecular docking studies (Fig. S1) on these molecules, we have identified two molecules with good binding energy using the MAP4K4 protein.

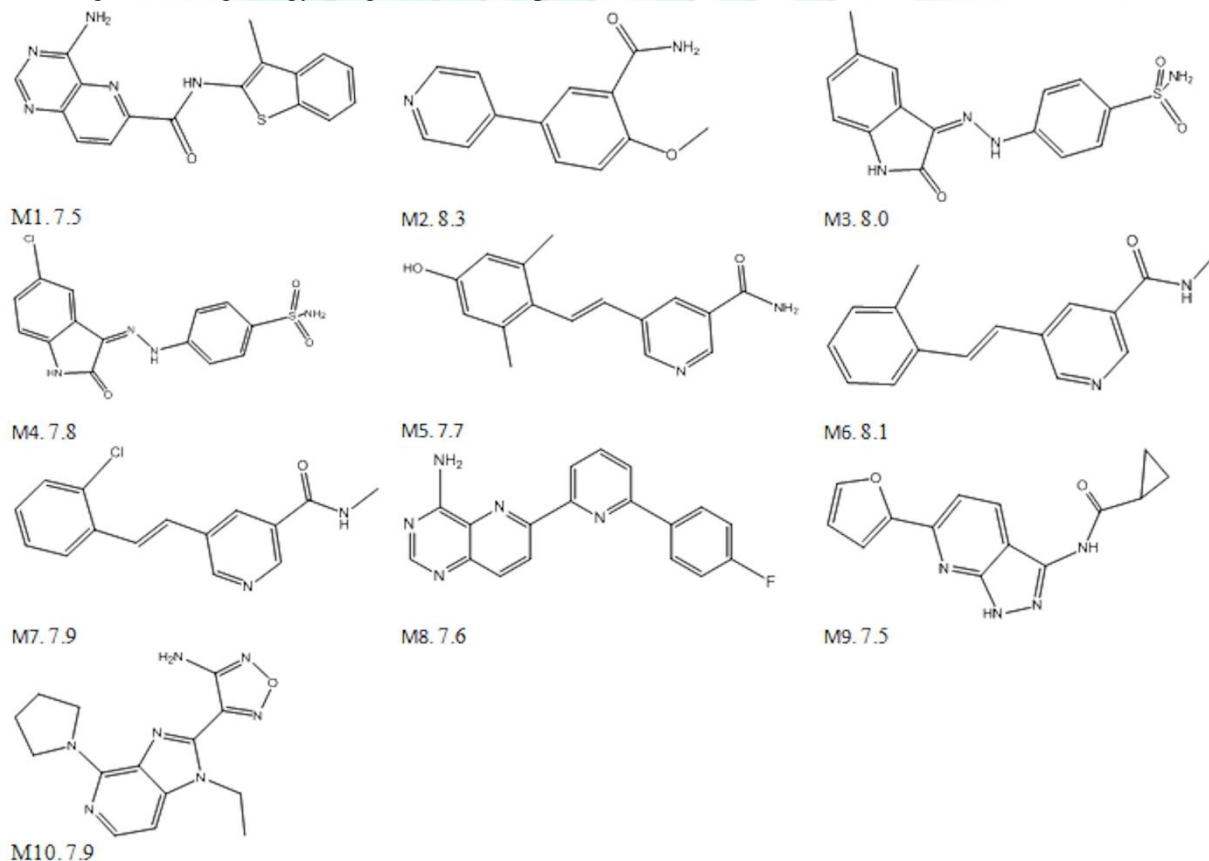


**Fig 3 :** The identified novel MAP4K4 inhibitor molecules using QSAR equation screening on GSK-PKIS database

### 3.2 Molecular docking:

The analogs of the pyridopyrimidine are docked into the ATP binding site of the MAP4K4. Molecules are showing good interactions with the active site residues. The pyridopyrimidine core is having hydrogen bonding with the hinge region of the

MAP4K4 protein. The hinge region of the MAP4K4 protein consists of the residues PHE-108, CYS-109, GLY-110 and ALA-111. The residues can form a hydrogen bond with the nitrogen and substituted  $\text{NH}_2$  of the pyridopyrimidine ring. There are two crystal structures available with the pyridopyrimidine analogs in the RCSB PDB database (PDB\_IDs: 4OBP and 4OBQ), and the core of the molecules also having the interactions with the hinge region. We considered similar orientation of the molecule in the binding site of MAP4K4. The fragments attached to the core ring were located in the deeper ATP binding pocket of the protein.

The molecular docking of low activity containing molecule-17 into the MAP4K4 active site reveals the binding of the molecule. The binding interactions and orientations are illustrated in Figure-4. The molecule-17 is having characteristic hydrogen bond between  $\text{NH}_2$  of the molecule with main chain carbonyl oxygen atom of GLU-107. Pyrimidine ring nitrogen is forming a hydrogen bond with the main-chain NH of the CYS-109 amino acid. The aromatic pyridopyrimidine ring of the inhibitor is stabilized by the side chain of LEU-161 residue.

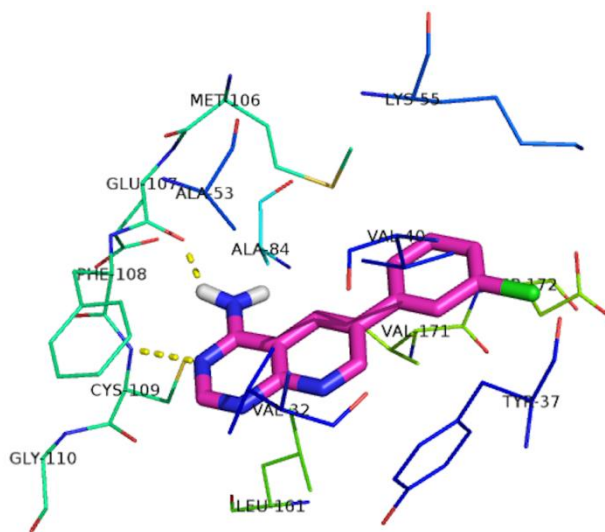


**Figure 4 :** The Molecular Docking of low activity molecule (Molecule 17) of training set into the active site of MAP4K4. The Molecule-17 is shown in stick model with magenta color. The protein amino acid side chains are shown in the residue type with the line model.

The molecule-25 is showing good activity and docked into the active site of the MAP4K4 protein. From the molecular docking studies, the molecule is showing strong hydrophilic and hydrophobic binding interactions and the orientation of the molecule is shown in fig. 5. The molecule amine group is making a hydrogen bond with the main chain carbonyl oxygen of GLU-107 amino acid. The nitrogen on the pyrimidine ring is forming a strong hydrogen bond with main-chain NH of the CYS-109 amino acid. The amide NH of the molecule is showing a hydrogen bond with ASP-172. This amide linker on dihydropyrrole moiety may be responsible for increasing the activity of the molecules. Fluoro-phenyl ring is stabilized by CH- $\pi$  interaction with VAL-40 residue.

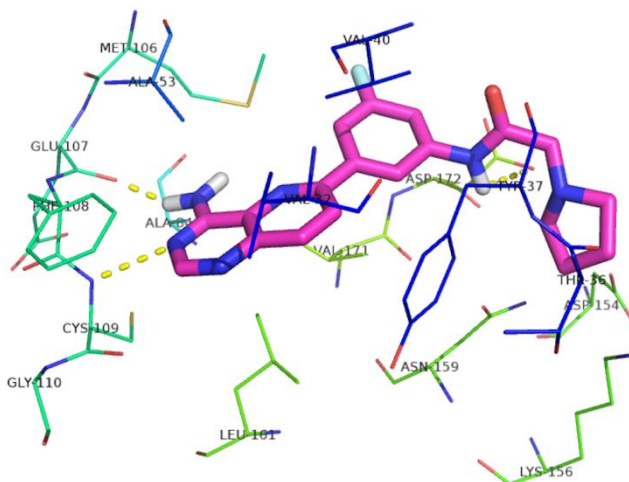


**Figure 5 :** Molecular docking of high activity containing molecule (molecule 25) of training set into the active site of the MAP4K4. The molecule-25 is shown in stick model with magenta color. The protein amino acid side chains are shown in the residue type with the line model.

The best QSAR model screening on GSK-PKIS database molecules resulted with two inhibitors M1 and M8 (shown in Fig. 3) with good predicted activity and also making good interactions with MAP4K4 protein during the molecular docking. These molecules are having hydrogen bonding with the hinge region residues. Molecules are showing strong hydrophobic interactions and the aromatic rings of the inhibitor molecules are forming CH- $\pi$  interactions with the side chains of the binding site residues.

The external set M1 molecule's NH is forming a hydrogen bond with the side chain hydroxyl group of Glu-107 and hydrophobic interactions with Val-40, Tyr-37 and Val-52 (shown in Fig. 6). The M8 molecule is forming two hydrogen bonds with the MAP4K4 active site. The amide NH of the M8 is forming a hydrogen bond with the side chain carboxylic group of Glu-107 and the ring N of the molecule is forming a hydrogen bond with the main chain NH of Cys-109. Further hydrophobic interactions with Val-40, Tyr-37 and Asn-159 (shown in Fig. 7).



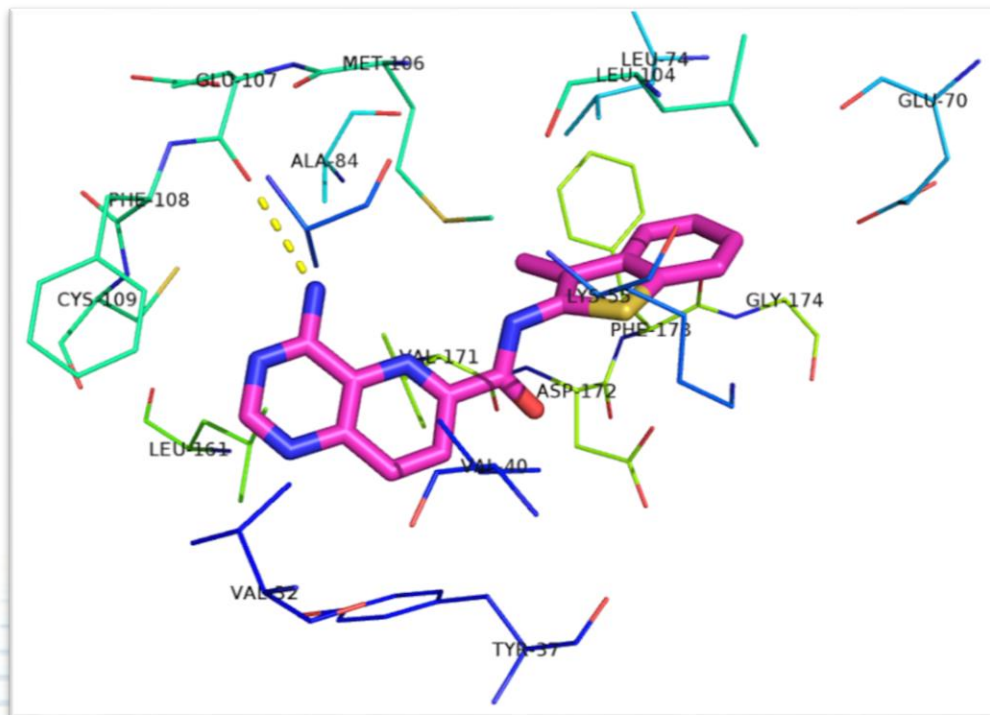


Figure 6 : Binding orientation of M1 showing good binding in the active site of MAP4K4 during molecular docking studies

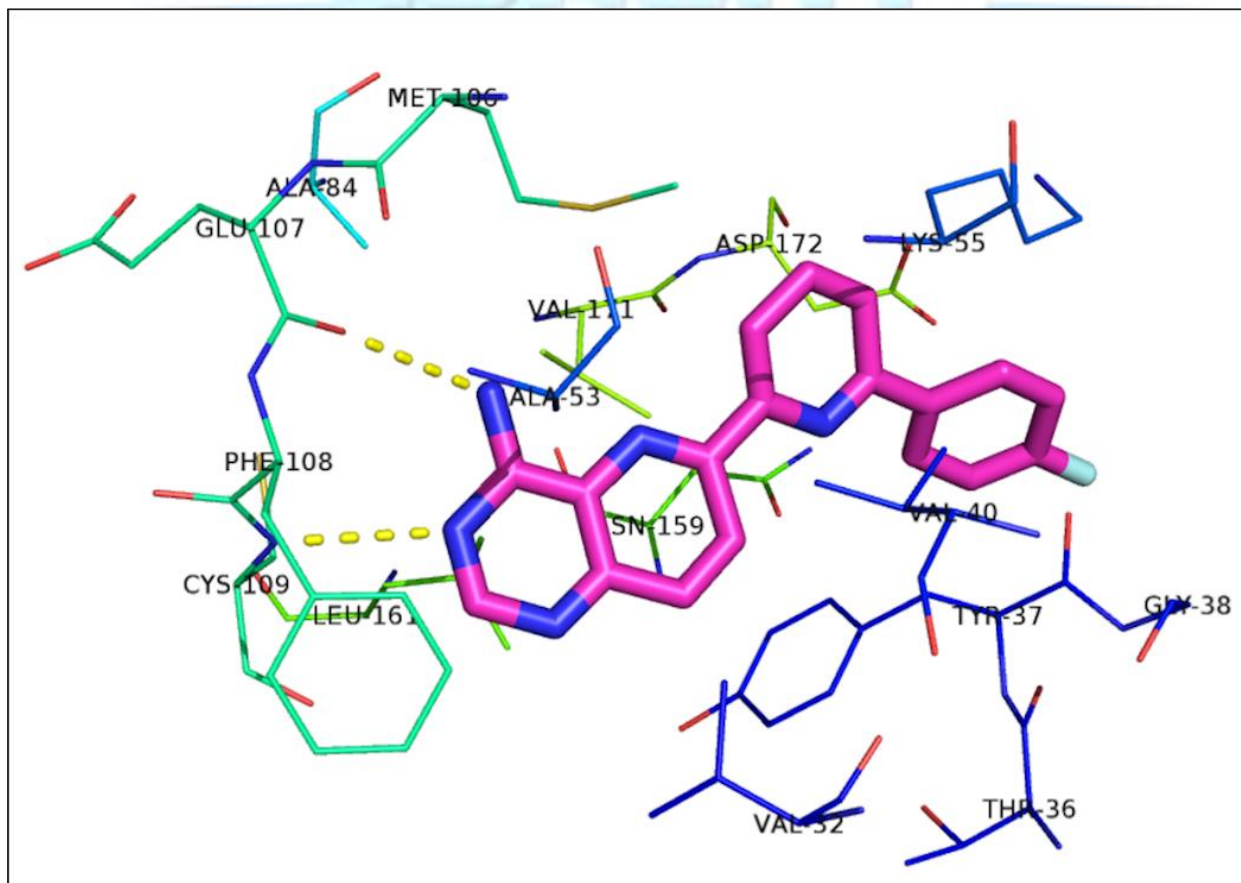
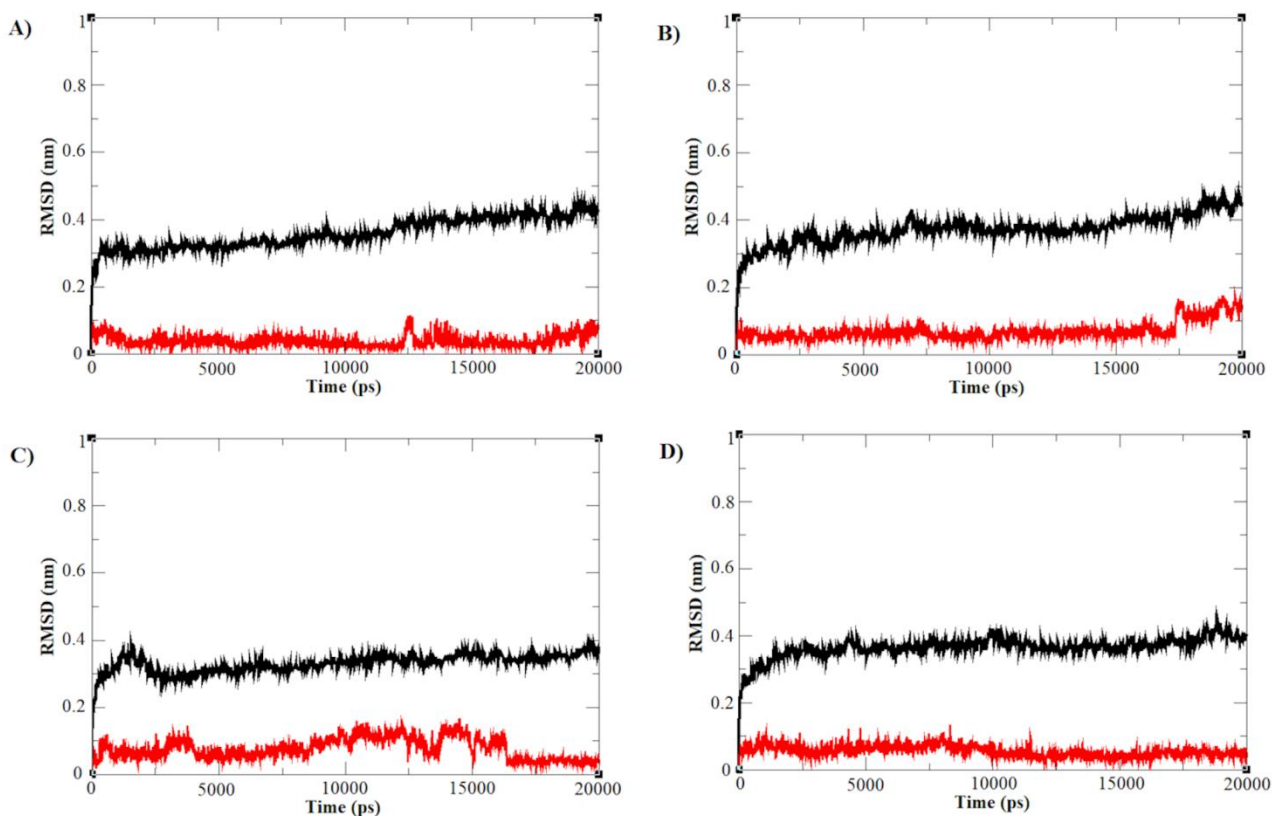


Figure 7 : Binding orientation of M8 is showing good binding in the active site of MAP4K4 during molecular docking studies



### 3.3 MD simulations and free energy calculations

A 20 nano seconds of MD simulations were performed on four complexes and the four molecules in MAP4K4 protein complexes were settled in their position in the active site during the simulations. The root-mean-square deviation (RMSD) plots of the ligand and proteins of four complexes were shown in Fig. 8. During the 15 to 20 ns of simulations time, the RMSD convergence was observed for both protein and ligand molecules. The convergence of the protein and ligand RMSD plot indicates the stability of the molecule in the active site of the protein. In all four RMSD plots the protein convergence appeared at 4 Å and the ligand converges observed at around 1 Å. The root-mean-square fluctuation (RMSF) plots of the four proteins were displayed in Fig. 9. The highly fluctuated region around at 1700 atom number in the plots is related to activation loop, and other small loop region fluctuations are also observed in the plots. The active site region residues of the protein and the other secondary structure elements are showing more stability during the simulations. Further, MMPBSA free energy calculations were performed using *g\_mmpbsa* on the trajectory of the complexes to understand the free energy binding. The molecule 17 with low pIC50 is showing the low binding free energy  $-113.28 \pm 1.43$  kJ/mol and the molecule 25 with high pIC50 is showing high binding free energy as  $-133.51 \pm 4.05$  kJ/mol respectively. The two predicted active molecules (M1 and M8 from Fig. 3) were showing the good binding free energies  $-125.78 \pm 7.91$  kJ/mol and  $-126.59 \pm 12.52$  kJ/mol respectively.



**Figure 8 :** RMSD plots of protein and ligand in complexes during 20 ns MD simulations of

A) Molecule 17., B) molecule 25.,

and the predicted active molecules RMSD is shown in C) Molecule M1 and D) Molecule M8. (Red– Ligand RMSD; Black – Protein RMSD)

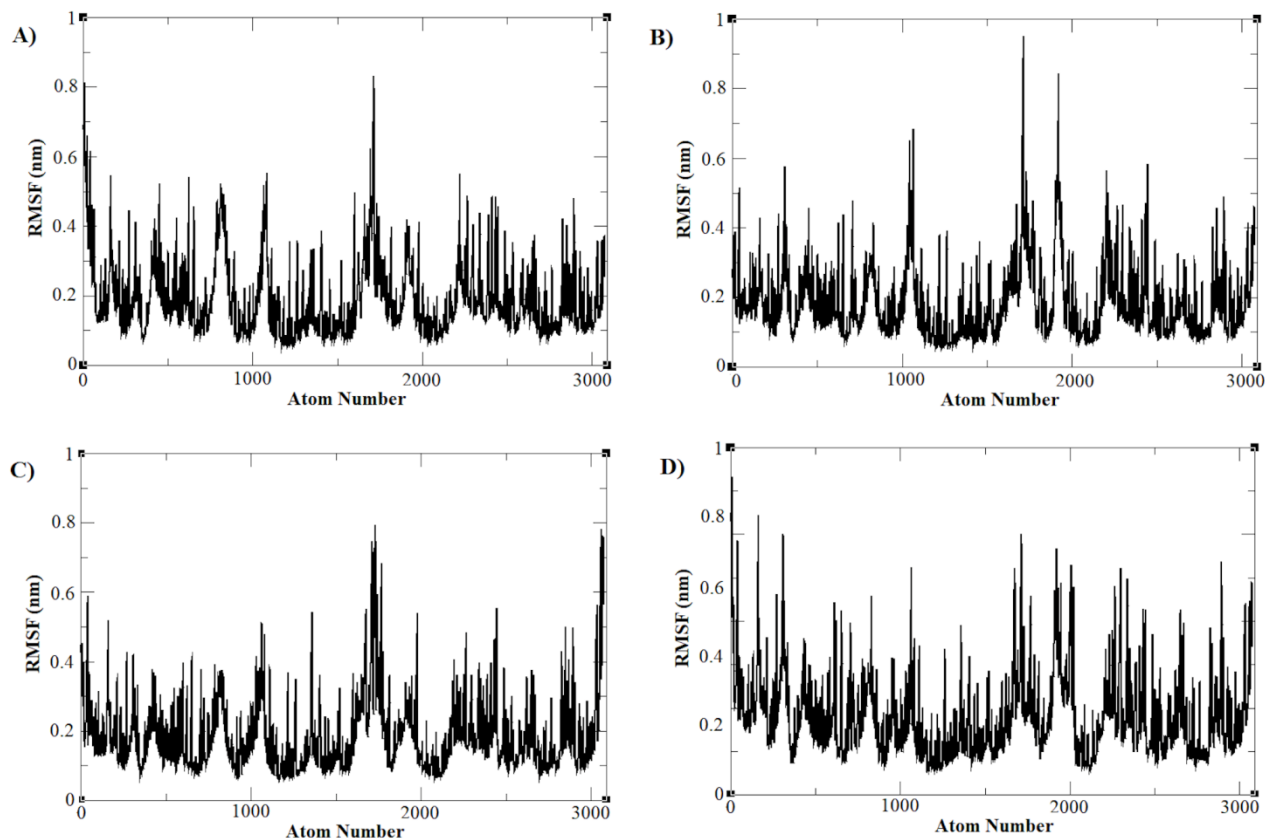


**Figure 9 :** RMSF plots of proteins in complexes during 20 ns MD simulations. A) Protein with molecule 17, B) protein with molecule 25, and the predicted active molecules RMSF is shown in C) protein with M1 D) protein with M8.

#### 4. Discussion

MAP4K4 kinase involvement was observed in the regulation of a number of biological processes, various cancers, angiogenesis, inflammation, and diabetes, and some of the significant work has been done on designing novel MAP4K4 inhibitors and in understanding its vital role in initial signalling pathways (Dow et al., 2018; Ndubaku et al., 2015; Ammirati et al., 2015; Schröder et al., 2015). The diverse substitutions on the phenyl ring of 6-phenylquinazolin-4-amine alter the activity of the molecules. The QSAR studies and molecular docking studies reveals that the electron donating mono substitution or electron withdrawing chlorine and fluorine on phenyl group are not much increasing the activity of the molecules. The amine group and the fluorine group as di- substitution slightly increasing the activity. The substituted amine on phenyl group with fluorine group is increasing the activity. Similarly the pyrido[3,2-d] pyrimidine ring containing molecules are also showing good activity. The crystal structure of MAP4K4 with pyridopyrimidine analogs in the PDB database (PDB\_IDs: 4OBP) reveals the core region interactions with the hinge region (Crawford et al., 2014). A cavity was formed with the residues from the kinase hinge region Cys108, Phe107, and Ploop Tyr36. Ndubaku et al. reported a structure based designed molecule GNE-495 with modified core from pyridopyrimidine to 1,7-naphthyridine scaffold increase the activity of the molecule against MAP4K4. (Ndubaku et al., 2015). The molecule 25 with the most active molecule in the data set is having the pyrido[3,2-d]pyrimidine ring showed strong hydrogen bond with the protein hinge region and the pyrrolidine ring is having strong hydrophobic interactions in the active site. The list of molecules screened against the best pharmacophore from the data also having good predicted pIC50 values. The pyridopyrimidine molecule derivatives are known for the MAP4K4 inhibitors (Crawford et al., 2014). Based on the substitutions, the activity changes were observed and the best QSAR model predictivity also comparable with the external data validation identifies the M1 and M8 molecules with pyrido[3,2-d] pyrimidine core moiety along the pyridine ring group substitutions resemble the training set molecules with good activity. This data support the predictivity of the generated best QSAR model and the other molecules in the external predicted molecules indole, imidazopyridine, pyrazolo pyridine and pyridine rings as core moieties. The substituted pyridine shows good predictive values and the selected external set table 2 contains three molecules with good predicted pIC50 values (Dow et al., 2018). Dow et al., developed a aminopyridine based core with 3- position substituted molecules and the incorporation of an oxyacetic acid

moiety was discussed for the MAP4K4 inhibitors to increase the potency and selectivity. They also discussed about the activity of the substitution at 2, 3 and 5 positions on pyridine (Dow et al., 2018). From the docking studies the hinge region of the protein is highly restricted by the hydrogen bonds from the inhibitor molecules was observed. The Val-40 Tyr-37 and Asp-172 residues are found in the deep cavity of the MAP4K4 protein. Further, from the simulations RMSF and RMSD plots we observed the overall MAP4K4 protein stabilized and mostly the active site regions are stable along with the inhibitor molecules. The consistency of the hinge region hydrogen bonds were observed throughout the simulations and the binding free energy of the molecules can be comparable with the actual and predicted activities. The more active molecules have good free energy and low active molecules have comparatively less free energy.

### 5. CONCLUSIONS

QSAR analysis of a total of 26 pyridopyrimidine analogs of MAP4K4 kinase ATP-competitive inhibitors have been carried out using Ezqsar and developed based on geometrical and topological descriptors to investigate the requirement for favorable receptor-inhibitor interactions. The best QSAR screening of GSK-PKIS database yielded with 10 molecules with good pIC50 values. From the molecular docking and molecular dynamics simulations studies, a hydrogen bond between the pyridopyrimidine ring and the hinge region residues was observed in all conformations with MAP4K4. With increasing the hydrophobic substitution like the amide linker, there is an increased activity of the molecules was observed.

### ACKNOWLEDGEMENT

We are thankful to the Department of Biotechnology, VFSTR Deemed to be University, Vadlamudi, for facilitating a work environment and thankful to the faculty for their encouragement and support.

### AUTHOR DISCLOSURE STATEMENT

There is no funding for this work.

### REFERENCES

- Ammirati, M., Bagley, S.W., Bhattacharya, S.K., et al. 2015. Discovery of an in vivo tool to establish proof of-concept for MAP4K4-based antidiabetic treatment. *ACS. Med. Chem. Lett.* 6, 1128-1133.
- Aouadi, M., Tesz, G.J., Nicoloso, S.M., et al. 2009. Orally delivered siRNA targeting macrophage Map4k4 suppresses systemic inflammation. *Nature.* 458, 1180-1184.
- Baker, N.A., Sept, D., Joseph, S., et al. 2001. Electrostatics of nanosystems: application to microtubules and the ribosome. *Proc. Natl. Acad. Sci. USA* 98, 10037-10041.
- Baumgartner, M., Sillman, A.L., Blackwood, E.M., et al. 2006. The Nck interacting kinase phosphorylates ERM proteins for formation of lamellipodium by growth factors. *Proc. Natl. Acad. Sci. USA* 103, 13391-13396.
- Bouzakri, K., Ribaux, P., Halban, P.A., 2009. Silencing mitogen-activated protein 4 kinase 4 (MAP4K4) protects beta cells from tumor necrosis factor-alpha-induced decrease of IRS-2 and inhibition of glucose stimulated insulin secretion. *J. Biol. Chem.* 284, 27892-27898.
- Bouzakri, K., Zierath, J.R., 2007. MAP4K4 gene silencing in human skeletal muscle prevents tumor necrosis factor-alpha-induced insulin resistance. *J. Biol. Chem.* 282, 7783-7789.
- Bussi, G., Donadio, D., Parrinello, M., 2007. Canonical sampling through velocityrescaling. *J. Chem. Phys.* 126, 014101.
- Chuang, H.C., Wang, X., Tan, T.H., 2016. MAP4K Family Kinases in Immunity and Inflammation. *Adv. Immunol.* 129, 277-314.
- Collins, C.S., Hong, J., Sapinoso, L., et al., 2006. A small interfering RNA screen for modulators of tumor cell motility identifies MAP4K4 as a promigratory kinase. *Proc. Natl. Acad. Sci. USA* 103, 3775-3780.
- Crawford, T.D., Ndubaku, C.O., Chen, H., et al. 2014 Discovery of selective 4-Amino-pyridopyrimidine inhibitors of MAP4K4 using fragment-based lead identification and optimization. *J. Med. Chem.* 57, 3484-3493.
- Delpire, E., 2009. The mammalian family of sterile 20p-like protein kinases. *Pflugers. Arch.* 458, 953-967.
- Dow, R.L., Ammirati, M., Bagley, S.W., et al. 2018. 2-Aminopyridine-Based Mitogen-Activated Protein Kinase Kinase Kinase 4 (MAP4K4) Inhibitors: Assessment of Mechanism-Based Safety. *J. Med. Chem.* 61, 3114-3125.
- Erlanson, D.A., 2011. *Introduction to Fragment-Based Drug Discovery. In Fragment-Based Drug Discovery and X-Ray Crystallography*; Topics in Current Chemistry, Springer: Berlin, Germany.
- Fan, Y., Shi, L.M., Kohn, K.W., et al., 2001 Quantitative structure-antitumor activity relationships of camptothecin analogues: cluster analysis and genetic algorithm based studies. *J. Med. Chem.* 44, 3254-3263.
- Gentleman, R.C., Carey, V.J., Bates, D.M., et al. 2004. Bioconductor: open software development for computational biology and bioinformatics. *Genome. Biol.* 5, R80.



- Hao, J.M., Chen, J.Z., Sui, H.M.Y., et al., 2010. A five-gene signature as a potential predictor of metastasis and survival in colorectal cancer. *J. Pathol.* 220, 475-489.
- Hess, B., Bekker, H., Berendsen, H.J.C., et al., 1997. LINCOS: a linear constraint solver for molecular simulations. *J. Comput. Chem.* 18, 1463-1472.
- Ihsan, M.F., Yanuar, A., 2018. Molecular dynamics simulations of several selected compounds from the herbal database of indonesia results of molecular docking against dna methyl transferase enzyme. *Int. J. App. Pharm.* 10, 285-290.
- KrishnamRaju, Ch., Shanmukha, K.J.V., GoudPalusa, S.K., 2018. Isolation and characterization of novel degradation products in cilnidipine by LC-QTOF-MS/MS, LCMSn, 2D-NMR and FTIR. *New. J. Chem.* 42, 634-646.
- Kumari, R., Kumar, R., 2014. Open Source Drug Discovery Consortium, Lynn A. g\_mmpbsa--a GROMACS tool for high-throughput MM-PBSA calculations. *J. Chem. Inf. Model.* 54, 1951-1962.
- Liang, J.J., Wang, H., Rashid, A., et al. 2008. Expression of MAP4K4 is associated with worse prognosis in patients with stage II pancreatic ductal adenocarcinoma. *Clin. Cancer. Res.* 14, 7043-7049.
- Liu, A.W., Cai, J., Zhao, X.L., et al., 2011. ShRNA-targeted MAP4K4 inhibits hepatocellular carcinoma growth. *Clin. Cancer. Res.* 17, 710-720.
- Loh, S.H., Francescut, L., Lingor, P., et al., 2007. Identification of new kinase clusters required for neurite outgrowth and retraction by a loss-of-function RNA interference screen. *Cell. Death. Differ.* 15, 283-298.
- Mao, J., Ligon, L., Rakhlin, E.Y., et al., 2006. A novel somatic mouse model to survey tumorigenic potential applied to the hedgehog pathway. *Cancer. Res.* 66, 10171-10178.
- Mehta, S., Pathak, S.R., 2017. Insilco drug design and molecular docking studies of novel coumarin derivatives as anti-cancer agents. *Asian. J. Pharm. Clin. Res.* 10, 335-340.
- Morris, G.M., Huey, R., Lindstrom, W., et al., 2009. Autodock4 and AutoDockTools4: automated docking with selective receptor flexibility. *J. Comp. Chem.* 16, 2785-2791.
- Muttaqin, F.Z., Fakhri, T.M., Muhammad, H.N., 2017. Molecular docking, molecular dynamics, and in silico toxicity prediction studies of coumarin, n-oxalylglycine, organoselenium, organosulfur, and pyridine derivatives as histone lysine demethylase inhibitors. *Asian. J. Pharm. Clin. Res.* 10, 212-215.
- Ndubaku, C.O., Crawford, T.D., Chen, H., et al. 2015. Structure-based design of GNE-495, a potent and selective MAP4K4 inhibitor with efficacy in retinal angiogenesis. *ACS. Med. Chem. Lett.* 6, 913-918.
- Parrinello, M., Rahman, A., 1981 Polymorphic transitions in single crystals: A new molecular dynamics method. *J. Appl. Phys.* 52, 7182-7190.
- Purushotham, U., Sastry, G.N., 2014. A comprehensive conformational analysis of tryptophan, its ionic and dimeric forms. *J. Comp. Chem.* 35, 595-610.
- Purushotham, U., 2018. Exploration of Conformations, Analysis of Protein and Biological Significance of Histidine Dimers. *Chem. Select.* 3, 3070-3078.
- Qiu, M.H., Qian, Y.M., Zhao, X.L., et al., 2012. Expression and prognostic significance of MAP4K4 in lung adenocarcinoma. *Pathol. Res. Pract.* 208, 541-548.
- R Core Team, 2013 R: a language and environment for statistical computing. R Foundation for Statistical Computing, Vienna, Austria. <http://www.R-project.org>.
- Rizzardi, A.E., Rosener, N.K., Koopmeiners, J.S., et al. 2014 Evaluation of protein biomarkers of prostate cancer aggressiveness. *BMC Cancer* 14, 244-258.
- Roy, K., Kar, S., Das, R., 2015. *QSAR/QSPR Modeling: Introduction. A Primer on QSAR/QSPR Modeling*, Springer International Publishing.
- Roy, K., Kar, S., Das, R., 2015. *Statistical methods in QSAR/QSPR. A Primer on QSAR/QSPR Modeling*, Springer International Publishing.
- Schröder, P., Förster, T., Kleine, S., et al. 2015. Neuritogenic militarinone-inspired 4-hydroxypyridones target the stress pathway kinase MAP4K4. *Angew. Chem. Int. Ed.* 54, 12398-12403.
- Shamsara, J., 2017. Ezqsar: An R Package for Developing QSAR Models Directly From Structures. *Open. Med. Chem. J.* 11, 212-221.
- Shanmukha, K. J. V., Prasanthi, S., Guravaiah, M., et al., 2012. Application of potassium permanganate to the spectrophotometric determination of oseltamivir phosphate in bulk and capsules. *Asian. J. Pharm. Clin. Res.* 5, 18-22.
- Steinbeck, C., Hoppe, C., Kuhn, S., et al., 2006. Recent developments of the chemistry development kit (CDK) - an open-source java library for chemo- and bioinformatics. *Curr. Pharm. Des.* 12, 2111-2120.
- Su, Y.C., Han, J., Xu, S., et al., 1997. NIK is a new Ste20-related kinase that binds NCK and MEKK1 and activates the SAPK/JNK cascade via a conserved regulatory domain. *EMBO J* 16, 1279-1290.
- Tang, X., Guilherme, A., Chakladar, A., et al., 2006. An RNA interference-based screen identifies MAP4K4/NIK as a negative regulator of PPARgamma, adipogenesis, and insulin-responsive hexose transport. *Proc. Natl. Acad. Sci. USA* 103, 2087-2092.



- Tanneeru, K., Reddy, B.M., Guruprasad, L., 2012. Three-dimensional quantitative structure–activity relationship (3D-QSAR) analysis and molecular docking of ATP-competitive triazine analogs of human mTOR inhibitors. *Med. Chem. Res.* 21, 1207-1217.
- Tanneeru, K., Sahu, I., Guruprasad, L., 2013. ligand based drug design of human endothelin converting enzyme-inhibitors. *Med. Chem. Res.* 22, 4401-4409.
- Todeschini, R., Ballabio, D., Grisoni, F., 2016. Beware of Unreliable Q(2)! A Comparative Study of Regression Metrics for Predictivity Assessment of QSAR Models. *J. Chem. Inf. Model.* 56, 1905-1913.
- Vadlakonda, R., Enaganti, S., Nerella, R., 2017. Insilco discovery of human aurora b kinase inhibitors by molecular docking, pharmacophore validation and ADMET studies. *Asian. J. Pharm. Clin. Res.* 10, 165-174.
- Van Der Spoel, D., Lindahl, E., Hess, B., et al., GROMACS: fast, flexible, and free. *J. Comput. Chem.* 26, 1701-1718.
- Veerasamy, R., Rajak, H., Jain, A., et al., 2011 Validation of QSAR Models - Strategies and Importance. *Int. J. Drug. Des. Discovery.* 2, 511-519.
- Wang, L., Stanley, M., Boggs, J.W., et al., 2014. Fragment-based identification and optimization of a class of potent pyrrolo[2,1-f][1,2,4]triazine MAP4K4 inhibitors. *Bioorg. Med. Chem. Lett.* 24, 4546-4552.
- Wright, J.H., Wang, X., Manning, G., et al., 2003. The STE20 kinase HGK is broadly expressed in human tumor cells and can modulate cellular transformation, invasion, and adhesion. *Mol. Cell. Biol.* 23, 2068-2082.
- Wu, C., Whiteway, M., Thomas, D.Y. et al., 1995. Molecular characterization of Ste20p, a potential mitogen-activated protein or extracellular signal-regulated kinase kinase (MEK) kinase kinase from *Saccharomyces cerevisiae*. *J. Biol. Chem.* 270, 15984-15992.

